Search for the weak decays J/ψ→D_{s}^{(*)−}e^{+}ν_{e}+c.c.

M. Ablikim *et al.* (BESIII Collaboration)

Phys. Rev. D **90**, 112014 — Published 23 December 2014

DOI: 10.1103/PhysRevD.90.112014

Search for the weak decays $J/\psi \to D_s^{(*)} e\nu_e$

M. Ablikim[1], M. N. Achasov[8,a], X. C. Ai[1], O. Albayrak[4], M. Albrecht[3], D. J. Ambrose[43], A. Amoroso[47A,47C], F. F. An[1], Q. An[44], J. Z. Bai[1], R. Baldini Ferroli[19A], Y. Ban[30], D. W. Bennett[18], J. V. Bennett[4], M. Bertani[19A], D. Bettoni[20A], J. M. Bian[42], F. Bianchi[47A,47C], E. Boger[22,g], O. Bondarenko[24], I. Boyko[22], R. A. Briere[4], H. Cai[49], X. Cai[1], O. Cakir[39A], A. Calcaterra[19A], G. F. Cao[1], S. A. Cetin[39B], J. F. Chang[1], G. Chelkov[22,b], G. Chen[1], H. S. Chen[1], H. Y. Chen[2], J. C. Chen[1], M. L. Chen[1], S. J. Chen[28], X. Chen[1], X. R. Chen[25], Y. B. Chen[1], H. P. Cheng[16], X. K. Chu[30], Y. P. Chu[1], G. Cibinetto[20A], D. Cronin-Hennessy[42], H. L. Dai[1], J. P. Dai[33], D. Dedovich[22], Z. Y. Deng[1], A. Denig[21], I. Denysenko[22], M. Destefanis[47A,47C], F. De Mori[47A,47C], Y. Ding[26], C. Dong[29], J. Dong[1], L. Y. Dong[1], M. Y. Dong[1], S. X. Du[51], P. F. Duan[1], J. Z. Fan[38], J. Fang[1], S. S. Fang[1], X. Fang[44], Y. Fang[1], L. Fava[47B,47C], F. Feldbauer[21], G. Felici[19A], C. Q. Feng[44], E. Fioravanti[20A], C. D. Fu[1], Q. Gao[1], Y. Gao[38], I. Garzia[20A], K. Goetzen[9], W. X. Gong[1], W. Gradl[21], M. Greco[47A,47C], M. H. Gu[1], Y. T. Gu[11], Y. H. Guan[1], A. Q. Guo[1], L. B. Guo[27], T. Guo[27], Y. Guo[1], Y. P. Guo[21], Z. Haddadi[24], A. Hafner[21], S. Han[49], Y. L. Han[1], F. A. Harris[41], K. L. He[1], Z. Y. He[29], T. Held[3], Y. K. Heng[1], Z. L. Hou[1], C. Hu[27], H. M. Hu[1], J. F. Hu[47A], T. Hu[1], Y. Hu[1], G. M. Huang[5], G. S. Huang[44], H. P. Huang[49], J. S. Huang[14], X. T. Huang[32], Y. Huang[28], T. Hussain[46], Q. Ji[1], Q. P. Ji[29], X. B. Ji[1], X. L. Ji[1], L. L. Jiang[1], L. W. Jiang[49], X. S. Jiang[1], J. B. Jiao[32], Z. Jiao[16], D. P. Jin[1], S. Jin[1], T. Johansson[48], A. Julin[42], N. Kalantar-Nayestanaki[24], X. L. Kang[1], X. S. Kang[29], M. Kavatsyuk[24], B. C. Ke[4], R. Kliemt[13], B. Kloss[21], O. B. Kolcu[39B,c], B. Kopf[3], M. Kornicer[41], W. Kuehn[23], A. Kupsc[48], W. Lai[1], J. S. Lange[23], M. Lara[18], P. Larin[13], C. H. Li[1], Cheng Li[44], D. M. Li[51], F. Li[1], G. Li[1], H. B. Li[1], J. C. Li[1], Jin Li[31], K. Li[12], K. Li[32], P. R. Li[40], T. Li[32], W. D. Li[1], W. G. Li[1], X. L. Li[32], X. M. Li[11], X. N. Li[1], X. Q. Li[29], Z. B. Li[37], H. Liang[44], Y. F. Liang[35], Y. T. Liang[23], G. R. Liao[10], D. X. Lin[13], B. J. Liu[1], C. L. Liu[4], C. X. Liu[1], F. H. Liu[34], Fang Liu[1], Feng Liu[5], H. B. Liu[11], H. H. Liu[15], H. H. Liu[1], H. M. Liu[1], J. Liu[1], J. P. Liu[49], J. Y. Liu[1], K. Liu[38], K. Y. Liu[26], L. D. Liu[30], Q. Liu[40], S. B. Liu[44], X. Liu[25], X. X. Liu[40], Y. B. Liu[29], Z. A. Liu[1], Zhiqiang Liu[1], Zhiqing Liu[21], H. Loehner[24], X. C. Lou[1,d], H. J. Lu[16], J. G. Lu[1], R. Q. Lu[17], Y. Lu[1], Y. P. Lu[1], C. L. Luo[27], M. X. Luo[50], T. Luo[41], X. L. Luo[1], M. Lv[1], X. R. Lyu[40], F. C. Ma[26], H. L. Ma[1], L. L. Ma[32], Q. M. Ma[1], S. Ma[1], T. Ma[1], X. N. Ma[29], X. Y. Ma[1], F. E. Maas[13], M. Maggiora[47A,47C], Q. A. Malik[46], Y. J. Mao[30], Z. P. Mao[1], S. Marcello[47A,47C], J. G. Messchendorp[24], J. Min[1], T. J. Min[1], R. E. Mitchell[18], X. H. Mo[1], Y. J. Mo[5], H. Moeini[24], C. Morales Morales[13], K. Moriya[18], N. Yu. Muchnoi[8,a], H. Muramatsu[42], Y. Nefedov[22], F. Nerling[13], I. B. Nikolaev[8,a], Z. Ning[1], S. Nisar[7], S. L. Niu[1], X. Y. Niu[1], S. L. Olsen[31], Q. Ouyang[1], S. Pacetti[19B], P. Patteri[19A], M. Pelizaeus[3], H. P. Peng[44], K. Peters[9], J. L. Ping[27], R. G. Ping[1], R. Poling[42], Y. N. Pu[17], M. Qi[28], S. Qian[1], C. F. Qiao[40], L. Q. Qin[32], N. Qin[49], X. S. Qin[1], Y. Qin[30], Z. H. Qin[1], J. F. Qiu[1], K. H. Rashid[46], C. F. Redmer[21], H. L. Ren[17], M. Ripka[21], G. Rong[1], X. D. Ruan[11], V. Santoro[20A], A. Sarantsev[22,e], M. Savrié[20B], K. Schoenning[48], S. Schumann[21], W. Shan[30], M. Shao[44], C. P. Shen[2], P. X. Shen[29], X. Y. Shen[1], H. Y. Sheng[1], M. R. Shepherd[18], W. M. Song[1], X. Y. Song[1], S. Sosio[47A,47C], S. Spataro[47A,47C], B. Spruck[23], G. X. Sun[1], J. F. Sun[14], S. S. Sun[1], Y. J. Sun[44], Y. Z. Sun[1], Z. J. Sun[1], Z. T. Sun[18], C. J. Tang[35], X. Tang[1], I. Tapan[39C], E. H. Thorndike[43], M. Tiemens[24], D. Toth[42], M. Ullrich[23], I. Uman[39B], G. S. Varner[41], B. Wang[29], B. L. Wang[40], D. Wang[30], D. Y. Wang[30], K. Wang[1], L. L. Wang[1], L. S. Wang[1], M. Wang[32], P. Wang[1], P. L. Wang[1], Q. J. Wang[1], S. G. Wang[30], W. Wang[1], X. F. Wang[38], Y. D. Wang[19A], Y. F. Wang[1], Y. Q. Wang[21], Z. Wang[1], Z. G. Wang[1], Z. H. Wang[44], Z. Y. Wang[1], D. H. Wei[10], J. B. Wei[30], P. Weidenkaff[21], S. P. Wen[1], U. Wiedner[3], M. Wolke[48], L. H. Wu[1], Z. Wu[1], L. G. Xia[38], Y. Xia[17], D. Xiao[1], Z. J. Xiao[27], Y. G. Xie[1], Q. L. Xiu[1], G. F. Xu[1], L. Xu[1], Q. J. Xu[12], Q. N. Xu[40], X. P. Xu[36], L. Yan[44], W. B. Yan[44], W. C. Yan[44], Y. H. Yan[17], H. X. Yang[1], L. Yang[49], Y. Yang[5], Y. X. Yang[10], H. Ye[1], M. Ye[1], M. H. Ye[6], J. H. Yin[1], B. X. Yu[1], C. X. Yu[29], H. W. Yu[30], J. S. Yu[25], C. Z. Yuan[1], W. L. Yuan[28], Y. Yuan[1], A. Yuncu[39B,f], A. A. Zafar[46], A. Zallo[19A], Y. Zeng[17], B. X. Zhang[1], B. Y. Zhang[1], C. Zhang[28], C. C. Zhang[1], D. H. Zhang[1], H. H. Zhang[37], H. Y. Zhang[1], J. J. Zhang[1], J. L. Zhang[1], J. Q. Zhang[1], J. W. Zhang[1], J. Y. Zhang[1], J. Z. Zhang[1], K. Zhang[1], L. Zhang[1], S. H. Zhang[1], X. J. Zhang[1], X. Y. Zhang[32], Y. Zhang[1], Y. H. Zhang[1], Z. H. Zhang[5], Z. P. Zhang[44], Z. Y. Zhang[49], G. Zhao[1], J. W. Zhao[1], J. Y. Zhao[1], J. Z. Zhao[1], Lei Zhao[44], Ling Zhao[1], M. G. Zhao[29], Q. Zhao[1], Q. W. Zhao[1], S. J. Zhao[51], T. C. Zhao[1], Y. B. Zhao[1], Z. G. Zhao[44], A. Zhemchugov[22,g], B. Zheng[45], J. P. Zheng[1], W. J. Zheng[32], Y. H. Zheng[40], B. Zhong[27], L. Zhou[1], Li Zhou[29], X. Zhou[49], X. K. Zhou[44], X. R. Zhou[44], X. Y. Zhou[1], K. Zhu[1], K. J. Zhu[1], S. Zhu[1], X. L. Zhu[38], Y. C. Zhu[44], Y. S. Zhu[1], Z. A. Zhu[1], J. Zhuang[1], B. S. Zou[1], J. H. Zou[1]

(BESIII Collaboration)

[1] *Institute of High Energy Physics, Beijing 100049, People's Republic of China*
[2] *Beihang University, Beijing 100191, People's Republic of China*
[3] *Bochum Ruhr-University, D-44780 Bochum, Germany*
[4] *Carnegie Mellon University, Pittsburgh, Pennsylvania 15213, USA*
[5] *Central China Normal University, Wuhan 430079, People's Republic of China*
[6] *China Center of Advanced Science and Technology, Beijing 100190, People's Republic of China*
[7] *COMSATS Institute of Information Technology, Lahore, Defence Road, Off Raiwind Road, 54000 Lahore, Pakistan*
[8] *G.I. Budker Institute of Nuclear Physics SB RAS (BINP), Novosibirsk 630090, Russia*
[9] *GSI Helmholtzcentre for Heavy Ion Research GmbH, D-64291 Darmstadt, Germany*
[10] *Guangxi Normal University, Guilin 541004, People's Republic of China*
[11] *GuangXi University, Nanning 530004, People's Republic of China*
[12] *Hangzhou Normal University, Hangzhou 310036, People's Republic of China*
[13] *Helmholtz Institute Mainz, Johann-Joachim-Becher-Weg 45, D-55099 Mainz, Germany*
[14] *Henan Normal University, Xinxiang 453007, People's Republic of China*

[15] Henan University of Science and Technology, Luoyang 471003, People's Republic of China
[16] Huangshan College, Huangshan 245000, People's Republic of China
[17] Hunan University, Changsha 410082, People's Republic of China
[18] Indiana University, Bloomington, Indiana 47405, USA
[19] (A)INFN Laboratori Nazionali di Frascati, I-00044, Frascati, Italy; (B)INFN and University of Perugia, I-06100, Perugia, Italy
[20] (A)INFN Sezione di Ferrara, I-44122, Ferrara, Italy; (B)University of Ferrara, I-44122, Ferrara, Italy
[21] Johannes Gutenberg University of Mainz, Johann-Joachim-Becher-Weg 45, D-55099 Mainz, Germany
[22] Joint Institute for Nuclear Research, 141980 Dubna, Moscow region, Russia
[23] Justus Liebig University Giessen, II. Physikalisches Institut, Heinrich-Buff-Ring 16, D-35392 Giessen, Germany
[24] KVI-CART, University of Groningen, NL-9747 AA Groningen, The Netherlands
[25] Lanzhou University, Lanzhou 730000, People's Republic of China
[26] Liaoning University, Shenyang 110036, People's Republic of China
[27] Nanjing Normal University, Nanjing 210023, People's Republic of China
[28] Nanjing University, Nanjing 210093, People's Republic of China
[29] Nankai University, Tianjin 300071, People's Republic of China
[30] Peking University, Beijing 100871, People's Republic of China
[31] Seoul National University, Seoul, 151-747 Korea
[32] Shandong University, Jinan 250100, People's Republic of China
[33] Shanghai Jiao Tong University, Shanghai 200240, People's Republic of China
[34] Shanxi University, Taiyuan 030006, People's Republic of China
[35] Sichuan University, Chengdu 610064, People's Republic of China
[36] Soochow University, Suzhou 215006, People's Republic of China
[37] Sun Yat-Sen University, Guangzhou 510275, People's Republic of China
[38] Tsinghua University, Beijing 100084, People's Republic of China
[39] (A)Ankara University, Dogol Caddesi, 06100 Tandogan, Ankara, Turkey; (B)Dogus University, 34722 Istanbul, Turkey; (C)Uludag University, 16059 Bursa, Turkey
[40] University of Chinese Academy of Sciences, Beijing 100049, People's Republic of China
[41] University of Hawaii, Honolulu, Hawaii 96822, USA
[42] University of Minnesota, Minneapolis, Minnesota 55455, USA
[43] University of Rochester, Rochester, New York 14627, USA
[44] University of Science and Technology of China, Hefei 230026, People's Republic of China
[45] University of South China, Hengyang 421001, People's Republic of China
[46] University of the Punjab, Lahore-54590, Pakistan
[47] (A)University of Turin, I-10125, Turin, Italy; (B)University of Eastern Piedmont, I-15121, Alessandria, Italy; (C)INFN, I-10125, Turin, Italy
[48] Uppsala University, Box 516, SE-75120 Uppsala, Sweden
[49] Wuhan University, Wuhan 430072, People's Republic of China
[50] Zhejiang University, Hangzhou 310027, People's Republic of China
[51] Zhengzhou University, Zhengzhou 450001, People's Republic of China

[a] Also at the Novosibirsk State University, Novosibirsk, 630090, Russia
[b] Also at the Moscow Institute of Physics and Technology, Moscow 141700, Russia and at the Functional Electronics Laboratory, Tomsk State University, Tomsk, 634050, Russia
[c] Currently at Istanbul Arel University, Kucukcekmece, Istanbul, Turkey
[d] Also at University of Texas at Dallas, Richardson, Texas 75083, USA
[e] Also at the PNPI, Gatchina 188300, Russia
[f] Also at Bogazici University, 34342 Istanbul, Turkey
[g] Also at the Moscow Institute of Physics and Technology, Moscow 141700, Russia

Using a sample of 2.25×10^8 J/ψ events collected with the BESIII detector at the BEPCII collider, we search for the J/ψ semi-leptonic weak decay $J/\psi \to D_s^- e^+ \nu_e + c.c.$ with a much higher sensitivity than previous searches. We also perform the first search for $J/\psi \to D_s^{*-} e^+ \nu_e + c.c.$ No significant excess of a signal above background is observed in either channel. At the 90% confidence level, the upper limits are determined to be $\mathcal{B}(J/\psi \to D_s^- e^+ \nu_e + c.c.) < 1.3 \times 10^{-6}$ and $\mathcal{B}(J/\psi \to D_s^{*-} e^+ \nu_e + c.c.) < 1.8 \times 10^{-6}$, respectively. Both are consistent with Standard Model predictions.

PACS numbers: 13.20.Gd, 14.40.Lb

I. INTRODUCTION

The J/ψ particle, lying below the open charm threshold, cannot decay into a pair of charmed mesons. However, the J/ψ can decay into a single charmed meson

via the weak interaction [1]. Weak decays of the J/ψ are rare processes, and the inclusive branching fractions of J/ψ decays to single D or D_s mesons are predicted to be of the order of 10^{-8} or less [2] in the Standard Model (SM). Figure. 1 shows the tree-level Feynman diagram within the SM for the decays $J/\psi \to D_s^{(*)} l\nu$ ($l = e$ or μ). Most recent theoretical calculations predict the $J/\psi \to D_s^{(*)} l\nu$ branching fractions to be $\simeq 10^{-10}$ by using quantum chromodynamics (QCD) sum rules and employing the covariant light-front quark model [3]. However, as mentioned in Refs. [4–7], the branching fractions of $J/\psi \to D(\bar{D})X$ (with X denoting any hadrons) could be enhanced when new interaction couplings are considered, such as in the top-color models, the Minimal Supersymmetric SM with R-parity violation, or the two-Higgs-doublet model. It is interesting to note that the ratio between $J/\psi \to D_s^* l\nu$ and $D_s l\nu$ is predicted to be $1.5 \sim 3.1$ in Ref. [2, 3], where part of the theoretical uncertainties cancel.

The BES collaboration has studied several weak decays, including semi-leptonic and non-leptonic weak decays of the J/ψ. With a 5.8×10^7 J/ψ events sample, the upper limit for $\mathcal{B}(J/\psi \to D_s^- e^+\nu_e + c.c.)$ was found to be 3.6×10^{-5} at the 90% confidence level (C.L.) [8], while the $J/\psi \to D_s^{*-} e^+\nu_e + c.c.$ has never been studied in experiments before. When we refer to $+c.c.$, we mean the combination of $J/\psi \to D_s^{(*)-} e^+\nu_e$ and the charge conjugated modes $J/\psi \to D_s^{(*)+} e^-\bar{\nu}_e$. In the following, the signals are the sum of both modes and charge conjugation is implied unless otherwise specified. Using a sample of 2.25×10^8 J/ψ events collected with the BESIII detector at the Beijing Electron Positron Collider (BEPCII) [9], we search for the weak decays $J/\psi \to D_s^- e^+\nu_e$ and $J/\psi \to D_s^{*-} e^+\nu_e$. The D_s^- meson is reconstructed via four decay modes: $D_s^- \to K^+K^-\pi^-$, $D_s^- \to K^+K^-\pi^-\pi^0$, $D_s^- \to K_S^0 K^-$, and $D_s^- \to K_S^0 K^+\pi^-\pi^-$, where the π^0 and K_S^0 mesons are reconstructed from their $\gamma\gamma$ and $\pi^+\pi^-$ decays, respectively. The D_s^* candidate is reconstructed from its radiative transitions to D_s. A 478 pb^{-1} data sample collected at the center-of-mass energy $\sqrt{s} = 4.009$ GeV [10] is used to study systematic uncertainties.

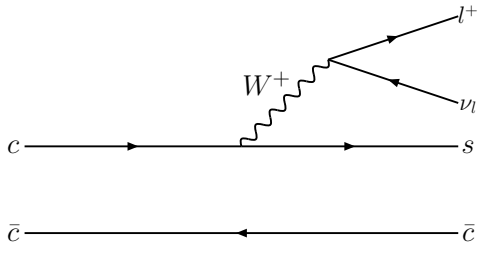

FIG. 1. Feynman diagrams for $J/\psi \to D_s^{(*)-} l^+\nu_l$ at the tree level.

II. THE BESIII EXPERIMENT

The BESIII detector is a magnetic spectrometer [11] located at BEPCII, which is a double-ring e^+e^- collider with a design peak luminosity of 10^{33} cm^{-2} s^{-1} at a center-of-mass energy of 3.773 GeV. The cylindrical core of the BESIII detector consists of a helium-based main drift chamber (MDC), a plastic scintillator time-of-flight system (TOF), and a CsI (Tl) electromagnetic calorimeter (EMC), which are all enclosed in a superconducting solenoidal magnet providing a 1.0 T magnetic field. The solenoid is supported by an octagonal flux-return yoke with modules of resistive plate muon counters interleaved with steel. The acceptance for charged particles and photons is 93% over a 4π solid angle. The momentum resolution for a charged particle at 1 GeV/c is 0.5%, and the ionization energy loss per unit path-length (dE/dx) resolution is 6%. The EMC measures photon energies with a resolution of 2.5% (5%) at 1 GeV in the barrel (end-caps). The time resolution for the TOF is 80 ps in the barrel and 110 ps in the end-caps.

Monte Carlo (MC) simulations are used to determine the detection efficiency, study backgrounds and optimize event selection criteria. A GEANT4-based [12] simulation is used to simulate the BESIII detector response. Electron-positron annihilation into a J/ψ resonance is simulated at energies around $\sqrt{s} = 3.097$ GeV, while the beam energy and its energy spread are set according to measurements of the Beam Energy Measurement System (BEMS) [13]. The production of the J/ψ resonance is implemented with the generator KKMC [14]. The signal channels are generated with a new generator implemented in EVTGEN [15], and we assume the process $J/\psi \to D_s^{(*)-} e^+\nu_e$ is dominated by the weak interaction, i.e. via the $c \to s$ charged current process, while the effects of hadronization and quark spin-flip are ignored. The known decay modes of the J/ψ resonance are generated by EVTGEN [15] with branching fractions set according to the world average values of the Particle Data Group (PDG) [16], while the unknown decays are generated by LUNDCHARM [17]. A sample of 2.25×10^8 generic J/ψ decays ('inclusive MC') is used to identify potential background channels.

III. EVENT SELECTION AND DATA ANALYSIS

Tracks from charged particles are reconstructed using hit information from the MDC. We select tracks in the polar angle range $|\cos\theta| < 0.93$ and require that they pass within ± 10 cm from the interaction point (IP) along the beam and within ± 1 cm transverse to the beam direction. The charged particle identification (PID) is based on a combination of dE/dx and TOF information, and the probability of each particle hypothesis ($P(i)$ with $i = e/\pi/K$) is calculated. A pion candidate is required to satisfy $P(\pi) > 0.001$ and $P(\pi) > P(K)$; for kaons,

$P(K) > 0.001$ and $P(K) > P(\pi)$ are required; and for electrons or positrons, we require the track from charged particles to satisfy $P(e) > 0.001$ and $P(e) > P(K)$ and $P(e) > P(\pi)$ as well as $0.80 < E/p < 1.05$, where E/p is the ratio of the energy deposited in the EMC to the momentum of the track measured by the MDC.

The K^0_S candidates are reconstructed from pairs of oppositely charged tracks, which are assumed to be pions without a PID requirement, and where the IP requirements are relaxed to 20 cm in the direction along the beam. For each pair of tracks, a primary vertex fit and a secondary vertex fit are performed and the K^0_S decay length is required to be 2 times larger than its fit error. The resulting track parameters from the secondary vertex fit are used to calculate the invariant mass $M(\pi^+\pi^-)$. The $\pi^+\pi^-$ combinations with an invariant mass $0.487\ \mathrm{GeV/c^2} < M(\pi^+\pi^-) < 0.511\ \mathrm{GeV/c^2}$ are kept as K^0_S candidates. Multiple K^0_S candidates are allowed in one event.

Photon candidates are reconstructed based on the showers in both the EMC barrel region ($|\cos\theta| < 0.8$) and the end-cap regions ($0.86 < |\cos\theta| < 0.92$). Showers from the barrel region must have a minimum energy of 25 MeV, while those in the end-caps must have at least 50 MeV. To exclude showers from charged particles, a photon candidate must be separated by at least 20° from any charged particle track with respect to the interaction-point. The EMC timing information ($0\ \mathrm{ns} \leqslant T \leqslant 700\ \mathrm{ns}$) is used to further suppress electronic noise and energy depositions unrelated to the event.

The π^0 candidates are reconstructed from pairs of photons. A kinematic fit is performed constraining the invariant mass of the photon pair to the known π^0 mass [16]. The combination with the minimum χ^2 from the kinematic fit that satisfies $\chi^2 < 100$, and $0.115\ \mathrm{GeV/c^2} < M(\gamma\gamma) < 0.150\ \mathrm{GeV/c^2}$ is kept for further analysis. The π^0 candidates with both photons from the end-cap regions are excluded due to poor resolution in this region of the detector.

With the previously described charged and neutral particle candidates, the D_s^- candidates can be reconstructed through the four decay modes mentioned in the introduction; we name them $KK\pi$, $KK\pi\pi$, K^0_SK and $K^0_SK\pi\pi$, and number each as the kth ($k = 1...4$) decay mode, in sequence. Since the resolution of the reconstructed D_s^- mass is different for each decay mode, the invariant mass of D_s^- candidates is required to be in different mass windows, which are taken as three times the respective resolution ($\pm 3\sigma$ around its central value). For $J/\psi \to D_s^{*-}e^+\nu_e$, the D_s^- and an additional photon candidate are combined to reconstruct D_s^{*-} candidates, and the invariant mass difference (ΔM) between $D_s^-\gamma$ and D_s^- is required to satisfy $0.125\ \mathrm{GeV/c^2} < \Delta M < 0.150\ \mathrm{GeV/c^2}$. In order to avoid bias, we set no requirement to select the best D_s^- or D_s^{*-} candidate, and multiple D_s^- or D_s^{*-} candidates are allowed in one event. According to the MC simulations, after all selection criteria are applied, events with multiple candidates occur in about 0.1% cases for each mode in $J/\psi \to D_s^-e^+\nu_e$ and about 0.2% for each mode in $J/\psi \to D_s^{*-}e^+\nu_e$. For real data, only a few events are observed and no events with multiple candidates are found, so the effect of the multiplicity of candidates can be safely ignored.

Once a D_s^- or D_s^{*-} is reconstructed, the signal event candidate is required to contain a positron track. Events that include charged particles other than those from the D_s^- and the positron candidate are vetoed. To reduce background contributions from mis-identified events with extra photons, we require the total energy of those extra neutral particles be less than 0.2 GeV or 0.3 GeV for D_s^- or D_s^{*-} in the modes of $K^+K^-\pi^-$, $K^0_SK^-$ and $K^0_SK^+\pi^-\pi^-$, respectively, and 0.15 GeV or 0.2 GeV for the $K^+K^-\pi^-\pi^0$ mode. These selection criteria are chosen by optimizing the ratio $S/\sqrt{B}$, where S and B are the numbers of signal events from the signal MC sample and expected background events from the inclusive MC sample, respectively.

For a $J/\psi \to D_s^{(*)-}e^+\nu_e$ candidate, the undetected neutrino leads to a missing energy $E_{miss} = E_{J/\psi} - E_{D_s^{(*)-}} - E_{e^+}$ and a missing momentum $\vec{p}_{miss} = \vec{p}_{J/\psi} - \vec{p}_{D_s^{(*)-}} - \vec{p}_{e^+}$, where $E_{D_s^{(*)-}}$ and $\vec{p}_{D_s^{(*)-}}$ (E_{e^+} and $\vec{p}_{e^+}$) are the energy and momentum of the $D_s^{(*)-}$ (positron). We require $|\vec{p}_{miss}|$ to be larger than 50 MeV to suppress the background contributions from J/ψ hadronic decays in which a pion is mis-identified as a positron. The J/ψ semileptonic decay events are extracted using the variable $U_{\rm miss} = E_{miss} - |\vec{p}_{miss}|$. If the decay products of the J/ψ semileptonic decay have been correctly identified, $U_{\rm miss}$ is expected to peak around zero. The $U_{\rm miss}$ distributions of $J/\psi \to D_s^-e^+\nu_e$ and $J/\psi \to D_s^{*-}e^+\nu_e$ candidates are shown in Figs. 2 and 3, respectively. The signal shapes obtained from MC simulations are shown with dashed curves. No significant excess of signal above background is observed in either mode.

From a MC study, we find that background events are mostly from those decay modes where a pion is mis-identified as an electron/positron. For example, the process $J/\psi \to K^+K^-\pi^-\pi^+$ would be one potential background of $J/\psi \to D_s^-e^+\nu_e$, $D_s^- \to K^+K^-\pi^-$. Background channels from inclusive MC simulations are shown in Figs. 2 and 3 with filled histograms. No peaking background is found, and the expected background from MC is consistent with data.

For each D_s^- decay mode, 100,000 exclusive signal MC events are generated, and the detection efficiencies are determined to be $(24.46 \pm 0.17)\%$, $(11.08 \pm 0.13)\%$, $(29.90 \pm 0.19)\%$ and $(13.74 \pm 0.12)\%$ for $KK\pi$, $KK\pi\pi^0$, K^0_SK and $K^0_SK\pi\pi$ modes of $J/\psi \to D_s^-e^+\nu_e$, and $(16.59 \pm 0.17)\%$, $(7.40 \pm 0.15)\%$, $(19.62 \pm 0.17)\%$ and $(8.20 \pm 0.11)\%$ for $KK\pi$, $KK\pi\pi^0$, K^0_SK and $K^0_SK\pi\pi$ modes of $J/\psi \to D_s^{*-}e^+\nu_e$, respectively.

A simultaneous unbinned maximum likelihood (ML) fit is used to determine the event yields of the four D_s decay modes. The Bayesian method [16] with a uniform prior is used to estimate the upper limits on the

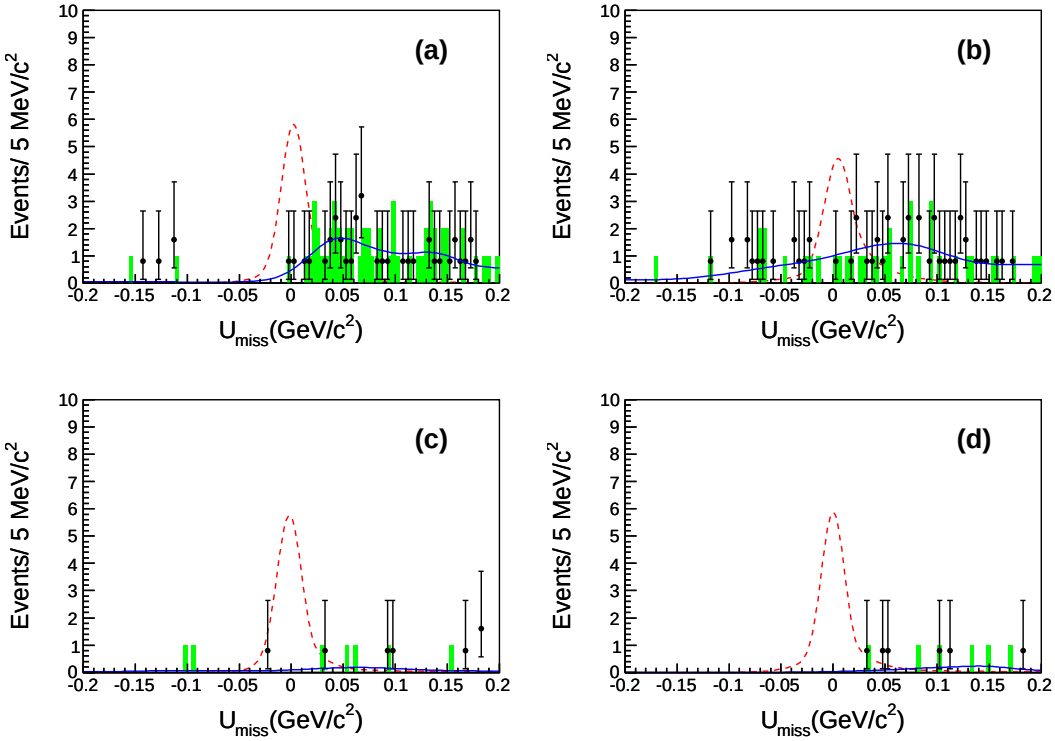

FIG. 2. $U_{\rm miss}$ distributions for $J/\psi \to D_s^- e^+ \nu_e$: (a) $D_s^- \to K^+K^-\pi^-$; (b) $D_s^- \to K^+K^-\pi^-\pi^0$; (c) $D_s^- \to K_S^0 K^-$; (d) $D_s^- \to K_S^0 K^+\pi^-\pi^-$. Data are shown by dots with error bars, the signal shapes are shown with dashed curves, the background contributions from inclusive MC simulations are shown with filled histograms, and the results of simultaneous fit are shown with solid curves. Here the signal shape is drawn with arbitrary normalization, while the shapes of inclusive MC and fit are normalized to the data luminosity.

number of signal events since no significant signals are observed for either J/ψ weak decay mode. We choose -0.2 GeV/c^2 $< U_{\rm miss} <$ 0.2 GeV/c^2 as the fitting range. The signal events are described by a sum of a Gaussian and a Crystal Ball function [18] with the parameters obtained from a fit to the signal MC sample. The background shape is obtained from the inclusive J/ψ MC sample and modeled with a probability density function that represents the shape of an external unbinned dataset as a superposition of Gaussians [19]. The likelihood for the kth D_s^- decay mode is constructed as:

$$\mathcal{L}_k = \prod_{i=1}^{N_k} \frac{N_{\rm total}\mathcal{B}_k\epsilon_k\mathcal{P}_{i,k}^{\rm sig} + N_k^{\rm bkg}\mathcal{P}_{i,k}^{\rm bkg}}{N_{\rm total}\mathcal{B}_k\epsilon_k + N_k^{\rm bkg}} \ , \qquad (1)$$

where $N_{\rm total}$ is the total number of produced $J/\psi \to D_s^{(*)-}e^+\nu_e$ events in data, $\mathcal{B}_k$ is the world average branching fraction of the kth D_s^- decay mode [16], ϵ_k is the detection efficiency of the kth D_s^- decay mode; $N_k^{\rm bkg}$ is the number of background events in the kth D_s^- decay mode. N_k is the total number of selected events in the fit region for the kth D_s^- decay mode. $\mathcal{P}_{i,k}^{\rm sig}$ is the probability density function of signal for the kth D_s^- decay mode evaluated at the ith event; similarly, $\mathcal{P}_{i,k}^{\rm bkg}$ is that of background. The total likelihood $\mathcal{L}$ is the product of likelihoods for each D_s^- decay mode. A simultaneous unbinned fit with floating amplitudes of signal and background is performed. No significant signal is found by the fit as expected, and the fitting results are shown in the Figs. 2 and 3 as solid curves.

We calculate the 90% C.L. upper limit yield from the fit, $N_{\rm total}^{\rm up}$, using

$$\frac{\int_0^{N_{\rm total}^{\rm up}} \mathcal{L}(N_{\rm total})dN_{\rm total}}{\int_0^{\infty} \mathcal{L}(N_{\rm total})dN_{\rm total}} = 0.90 \ , \qquad (2)$$

where $\mathcal{L}(N_{\rm total})$ is the total likelihood $\mathcal{L}$ at fixed $N_{\rm total}$.

In each fit, the likelihood value is obtained and the corresponding probabilities are calculated as shown in Fig. 4. Figure. 4 also shows the numbers of $N_{\rm total}$ corresponding to 90% of the accumulated areas below the likelihood curves, which are then quoted as the upper limits on the number of signal events at the 90% C.L. The limits are 244 and 335 for the $J/\psi \to D_s^- e^+\nu_e$ and $J/\psi \to D_s^{*-} e^+\nu_e$ decay modes, respectively.

IV. SYSTEMATIC UNCERTAINTIES

Systematic uncertainties in this analysis are divided into two sets. The dominant one is from the uncer-

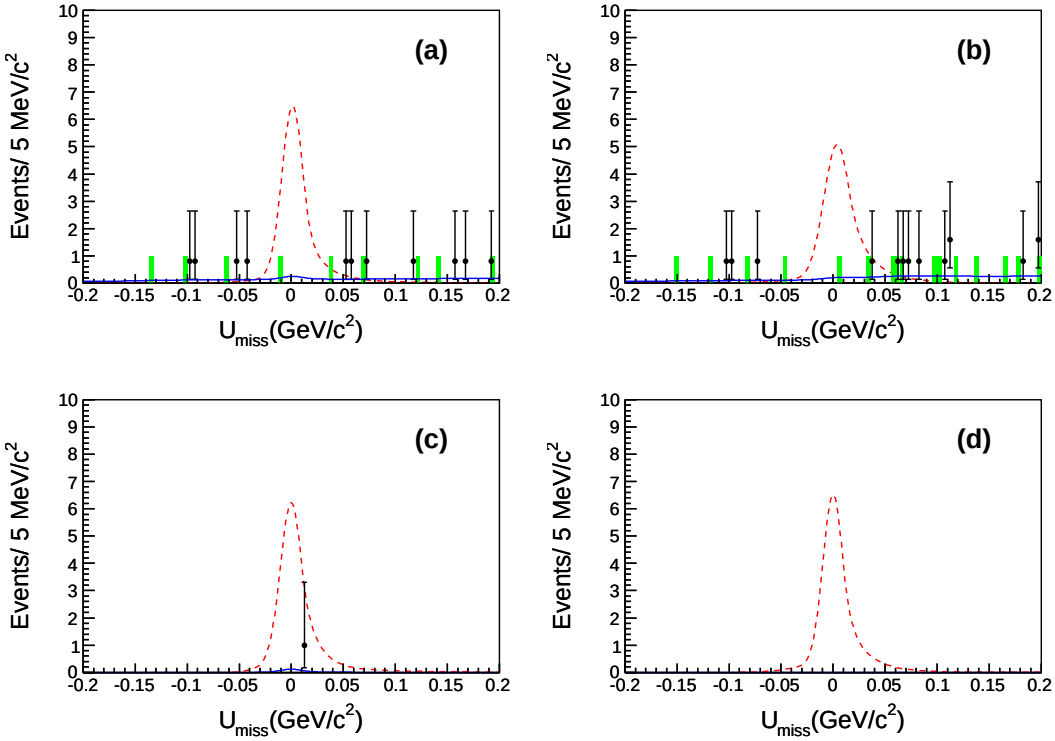

FIG. 3. $U_{\rm miss}$ distributions for $J/\psi \to D_s^{*-}e^+\nu_e$: (a) $D_s^- \to K^+K^-\pi^-$; (b) $D_s^- \to K^+K^-\pi^-\pi^0$; (c) $D_s^- \to K_S^0K^-$; (d) $D_s^- \to K_S^0K^+\pi^-\pi^-$. Data are shown by dots with error bars, the signal shapes are shown with dashed curves, the background contributions from inclusive MC simulations are shown with filled histograms, and the results of simultaneous fit are shown with solid curves. Here the signal shape is drawn with arbitrary normalization, while the shapes of inclusive MC and fit are normalized with to the data luminosity.

tainty of the efficiency corrected signal yield. The others are common uncertainties, including physics model, electron tracking, electron PID, E/p cut, the total number of J/ψ events, and the trigger efficiency, as well as the photon efficiency and $\mathcal{B}(D_s^{*-} \to D_s^-\gamma)$ for D_s^* mode.

A. Systematic uncertainty of efficiency corrected signal yield for each channel

The systematic uncertainties caused by charged and neutral particle reconstruction efficiencies, K and π PID efficiencies, the π^0 reconstruction efficiency, the K_S^0 reconstruction efficiency, and D_s mass resolutions are all considered together as the systematic error due to the reconstruction efficiency of the D_s. It is the dominant uncertainty in this analysis and is studied using a control sample of $\psi(4040) \to D_s^+D_s^-$, in which a 478 pb^{-1} $\psi(4040)$ data sample taken at 4.009 GeV is used [10]. In this study, one D_s is tagged using eight D_s hadronic decays modes, and the other D_s is reconstructed in the same way as in the $J/\psi \to D_s^{(*)-}e^+\nu_e$ analysis. The differences of the D_s reconstruction efficiencies of MC and data are quoted as the systematic uncertainties in the D_s reconstruction and are listed in Tabs. I and II. The uncertainties on the D_s decay branching fractions are separated from the reconstruction uncertainty deliberately by squared subtraction.

The systematic uncertainty of background shapes is estimated by varying the shapes of background. These new background shapes are obtained by smoothing the bin contents of the histograms, that are extracted from the inclusive MC sample. By convolution with a Guassian function, we repeat this process till the maximum difference between the contents of any two adjacent bins is less than 25%.

The systematic uncertainty due to the choice of fitting ranges is determined by varying the ranges of the $U_{\rm miss}$ distributions from $[-0.2, 0.2]$ GeV/c^2 to $[-0.25, 0.25]$ GeV/c^2, and the difference is taken as this systematic uncertainty.

The systematic uncertainty contributions studied above and the uncertainty due to MC statistics are summarized in Tables I and II. The total uncertainty is obtained by summing in quadrature the individual uncertainties quadratically.

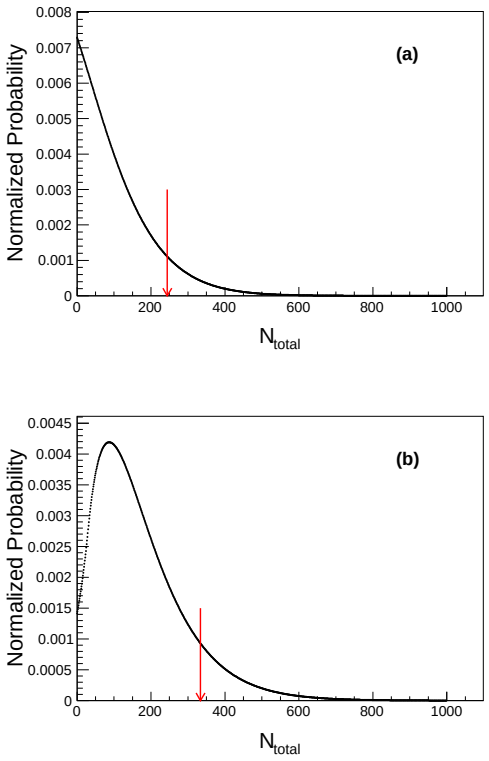

FIG. 4. Normalized probabilities as a function of $N_{\rm total}$ in the (a) $J/\psi \to D_s^- e^+ \nu_e$ and (b) $J/\psi \to D_s^{*-} e^+ \nu_e$ decay modes. The red arrows indicate where 90% of the area is accumulated below the curves.

TABLE I. Summary of systematic uncertainties of the efficiency corrected signal yield in the measurement of $J/\psi \to D_s^- e^+ \nu_e$ in %.

Sources\modes	$K^+K^-\pi^-$	$K^+K^-\pi^-\pi^0$	$K_S^0K^-$	$K_S^0K^-\pi^+\pi^-$
reconstruction ϵ	6.8	16.2	16.6	18.6
$\mathcal{B}(D_s^- \to X)$	3.9	11.1	4.0	6.6
background shape	2.3	2.4	3.2	2.9
fitting range	0.3	0.4	0.5	0.6
MC statistic	0.7	1.2	0.6	0.9
total	8.2	19.8	17.4	20.0

TABLE II. Summary of systematic uncertainties of the efficiency corrected signal yield in the measurement of $J/\psi \to D_s^{*-} e^+ \nu_e$ in %.

Sources\modes	$K^+K^-\pi^-$	$K^+K^-\pi^-\pi^0$	$K_S^0K^-$	$K_S^0K^-\pi^+\pi^-$
reconstruction ϵ	6.8	16.2	16.6	18.6
$\mathcal{B}(D_s^- \to X)$	3.9	11.1	4.0	6.6
background shape	2.5	2.5	2.7	3.2
fitting range	0.2	0.6	0.4	0.4
MC statistic	1.0	1.9	0.9	1.4
total	8.3	20.0	17.4	20.1

B. Common uncertainties

The difference of the efficiencies based on phase space (PHSP) and the new generator used in this analysis is taken as the systematic uncertainty of the physics model.

The systematic uncertainty of the resolutions has been estimated by smearing the MC simulations. The simulation of the photon reconstruction has been studied with a control sample of the well understood decays $J/\psi \to \rho^0\pi^0$ in Ref. [20], and we smear the resolution of the photon energy deposited in the EMC at the 1% level by a convolution with a Gaussian function. For the tracks from charged particles, we smear the helix parameters of each track as described in Ref. [21]. The difference in the final yields between before and after smearing is taken as the systematic uncertainty. The variable $U_{\rm miss}$ is associated with the energy and momentum resolutions of detected tracks. Thus, the systematic uncertainty of the signal shape has been taken into account implicitly.

The electrons from the signal are in a low momentum region, which cause a systematic uncertainty of 2.1% in the MDC tracking efficiency and 1.0% in the PID efficiency [22]. A radiative Bhabha sample, normalized with respect to the momentum, is used as a control sample to estimate the systematic uncertainty caused by the E/p requirement, i.e. $0.80 < E/p < 1.05$. The difference in efficiency between the MC simulation and the data is quoted as the systematic uncertainty caused by this requirement. Since the electron momentum in the $J/\psi \to D_s^{*-} e^+ \nu_e$ decay is lower, the uncertainty caused by the E/p requirement of $J/\psi \to D_s^{*-} e^+ \nu_e$ is larger than that of $J/\psi \to D_s^- e^+ \nu_e$ correspondingly.

The total number of J/ψ events is determined by using J/ψ inclusive decays [9], and the value 1.2% is quoted as the systematic uncertainty of the total number of J/ψ events.

According to Ref. [23], the trigger efficiency is very high since there are four to six tracks from charged particles in addition to possible neutral particles within the barrel regions in the final states. Therefore, the systematic uncertainty of the trigger efficiency is negligible.

Since the D_s^* mesons are only reconstructed by $D_s^{*-} \to D_s^-\gamma$, we deal with most of the systematic uncertainties of $J/\psi \to D_s^{*-} e^+ \nu_e$ in the same way as those of $J/\psi \to D_s^- e^+ \nu_e$, and with two additional uncertainties in D_s^* than in the D_s mode. One is a 1% uncertainty from the additional photon detecting efficiency [24]. The other one is the input branching fraction $\mathcal{B}(D_s^{*-} \to D_s^-\gamma)$ in MC simulation. Since the world average value is $(94.2 \pm 0.7)\%$ [16], this leads to a 0.7% uncertainty. All of the common systematic uncertainties are listed in Table III.

C. Upper limit calculation

Taking the systematic uncertainties into account, the upper limits on the branching fractions are calculated

TABLE III. Summary of common systematic uncertainties in the measurement of $J/\psi \to D_s^- e^+ \nu_e$ and $J/\psi \to D_s^{*-} e^+ \nu_e$.

Source	$J/\psi \to D_s^- e^+ \nu_e$ (%)	$J/\psi \to D_s^{*-} e^+ \nu_e$ (%)
physics model	0.9	0.8
resolutions	1.6	1.8
e tracking	2.1	2.1
e PID	1.0	1.0
E/p cut	0.6	1.7
photon efficiency	-	1.0
$\mathcal{B}(D_s^{*-} \to D_s^- \gamma)$	-	0.7
J/ψ events	1.2	1.2
trigger	negligible	negligible
total	3.3	3.9

TABLE IV. Upper limits of the branching fractions of $J/\psi \to D_s^- e^+ \nu_e$ and $J/\psi \to D_s^{*-} e^+ \nu_e$ after considering the systematic uncertainties.

	$J/\psi \to D_s^- e^+ \nu_e$	$J/\psi \to D_s^{*-} e^+ \nu_e$
$N^{\rm up}_{\rm total}$	244	335
$\sigma_{\rm total}$	31	43
$N^{\rm up\ \prime}_{\rm total}$	275	378
$\sigma^{\rm sys}_{\rm common}$	3.3%	3.9%
$N_{J/\psi}$	2.25×10^8	
$\mathcal{B}$(90%C.L.)	$< 1.3 \times 10^{-6}$	$< 1.8 \times 10^{-6}$

using

$$\mathcal{B} < \frac{N^{\rm up\ \prime}_{\rm total}}{(1-\sigma^{\rm sys}_{\rm common})N_{J/\psi}} \quad , \tag{3}$$

where $N^{\rm up\ \prime}_{\rm total}$ is the corrected $N^{\rm up}_{\rm total}$ after considering the systematic uncertainties of the signal efficiency, as described below, and $\sigma^{\rm sys}_{\rm common}$ is the total common systematic uncertainty.

From Eqs. 1 and 2, $N^{\rm up}_{\rm total}$ depends on the signal efficiencies of all decay channels in a complex way, and there is no simple analytic method to calculate the final effect due to those efficiency uncertainties. To study this dependence, we obtain an $N^{\rm up}_{\rm total}$ distribution by sampling each signal efficiency by a Gaussian function whose mean value and standard deviation are set as the normal signal efficiency and the systematic uncertainty obtained before, respectively. This new $N^{\rm up}_{\rm total}$ distribution can be described by a Gaussian function too, then a sum of the mean value ($N^{\rm up}_{\rm total}$) and one standard deviation ($\sigma_{\rm total}$) of this Gaussian function is quoted as the $N^{\rm up\ \prime}_{\rm total}$. All the numerical results are summarized in Table IV.

V. SUMMARY

With a sample of 2.25×10^8 J/ψ events collected with the BESIII detector, we have searched for the weak decays $J/\psi \to D_s^- e^+ \nu_e$ and $J/\psi \to D_s^{*-} e^+ \nu_e$. No significant excess of signal is observed. At the 90% C.L., the upper limits of the branching fractions are: $\mathcal{B}(J/\psi \to D_s^- e^+ \nu_e + c.c.) < 1.3 \times 10^{-6}$ and $\mathcal{B}(J/\psi \to D_s^{*-} e^+ \nu_e + c.c.) < 1.8 \times 10^{-6}$. The upper limit on the branching fraction $\mathcal{B}(J/\psi \to D_s^{*-} e^+ \nu_e + c.c.)$ is set for the first time and the upper limit on the branching fraction $\mathcal{B}(J/\psi \to D_s^- e^+ \nu_e + c.c.)$ is 30 times more strict than the previously result [16]. The results are within the SM prediction, but more data will be helpful to test the branching fraction of semileptonic decays of the J/ψ to the order of 10^{-8}. The results would also be applied to constrain the parameter spaces of some BSM models if direct calculations of these processes are carried out in the future.

ACKNOWLEDGEMENT

The BESIII collaboration thanks the staff of BEPCII and the IHEP computing center for their strong support. This work is supported in part by National Key Basic Research Program of China under Contract No. 2015CB856700; Joint Funds of the National Natural Science Foundation of China under Contracts Nos. 11079008, 11179007, U1332201; National Natural Science Foundation of China (NSFC) under Contracts Nos. 10625524, 10821063, 10835001, 11125525, 11235011, 11335008; the Chinese Academy of Sciences (CAS) Large-Scale Scientific Facility Program; CAS under Contracts Nos. KJCX2-YW-N29, KJCX2-YW-N45; 100 Talents Program of CAS; German Research Foundation DFG under Contract No. Collaborative Research Center CRC-1044; Istituto Nazionale di Fisica Nucleare, Italy; Ministry of Development of Turkey under Contract No. DPT2006K-120470; National Natural Science Foundation of China (NSFC) under Contract No. 11275189; Russian Foundation for Basic Research under Contract No. 14-07-91152; U. S. Department of Energy under Contracts Nos. DE-FG02-04ER41291, DE-FG02-05ER41374, DE-FG02-94ER40823, DESC0010118; U.S. National Science Foundation; University of Groningen (RuG) and the Helmholtzzentrum fuer Schwerionenforschung GmbH (GSI), Darmstadt; WCU Program of National Research Foundation of Korea under Contract No. R32-2008-000-10155-0.

[1] M. A. Sanchis, Phys. Lett. B **280**, 299 (1992).
[2] M. A. Sanchis-Lozano, Z. Phys. C **62**, 271 (1994).
[3] Y. -M. Wang, H. Zou, Z. -T. Wei, X. -Q. Li and C. -D. Lu, Eur. Phys. J. C **54**, 107 (2008).
[4] Xinmin Zhang, High Energy Phys. Nucl. Phys. **25**, 461 (2001).
[5] H. -B. Li and S. -H. Zhu, Chin. Phys. C **36**, 932 (2012).
[6] A. Datta, P. J. O'Donnell, S. Pakvasa and X. Zhang, Phys. Rev. D **60**, 014011 (1999).
[7] C. Hill, Phys. Lett. B **345**, 483 (1995).
[8] M. Ablikim *et al.* [BES Collaboration], Phys. Lett. B **639**, 418 (2006).
[9] M. Ablikim *et al.* [BESIII Collaboration], Chin. Phys. C **36**, 915 (2012).
[10] M. Ablikim *et al.* [BESIII Collaboration], Phys. Rev. D **86**, 071101 (2012).
[11] M. Ablikim *et al.* [BESIII Collaboration], Nucl. Instrum. Meth. A **614**, 345 (2010).
[12] S. Agostinelli *et al.* [GEANT4 Collaboration], Nucl. Instrum. Meth. A **506**, 250 (2003).
[13] E. V. Abakumova, M. N. Achasov, V. E. Blinov*et al.*, Nucl. Instrum. Meth. A **659**, 21 (2011).
[14] S. Jadach, B. F. L. Ward and Z. Was, Comp. Phys. Commu. **130**, 260 (2000); S. Jadach, B. F. L. Ward and Z. Was, Phys. Rev. D **63**, 113009 (2001).
[15] D. J. Lange, Nucl. Instrum. Meth. A **462**,152 (2001).
[16] K.A. Olive *et al.* [Particle Data Group], Chin. Phys. C, **38**, 090001 (2014).
[17] R. G. Ping *et al.* , Chin. Phys. C **32**, 599 (2008).
[18] J. Gaiser, SLAC Stanford - SLAC-255 (82,REC.JUN.83) 194p.
[19] K. S. Cranmer, Comput. Phys. Commun. **136**, 198 (2001).
[20] M. Ablikim *et al.* [BESIII Collaboration], Phys. Rev. D **81**, 052005 (2010).
[21] M. Ablikim *et al.* [BESIII Collaboration], Phys. Rev. D **87**, 012002 (2013).
[22] M. Ablikim *et al.* [BESIII Collaboration], Phys. Rev. D **87**, 092011 (2013).
[23] N. Berger, K. Zhu *et al.*, Chin. Phys. C **34**, 1779 (2010).
[24] M. Ablikim *et al.* [BESIII Collaboration], Phys. Rev. D **83**, 112005 (2011).